Climate Dynamics manuscript No.
(will be inserted by the editor)

Characteristics and development of European cyclones with tropical origin

Mark Dekker · Rein Haarsma · Hylke de Vries · Michiel Baatsen · Aarnout van Delden

Received: date / Accepted: date

Abstract Using the Modern-Era Retrospective analysis for Research and Applications (MERRA) reanalysis data set for the period 1979-2013, the characteristics of cyclones originating from the tropics that reach western Europe have been analyzed. Four different life cycles have been identified, that differ in structure during the tropical phase, extratropical transition and final development when they reach Europe. The strongest storms that reach Europe are warm seclusion cyclones. They are characterized by a warm core and a frontal T-bone structure. Rapid deepening occurs in the latest phase, around their arrival in Europe. A recent modeling study that has been reported earlier suggests that warm seclusion storms might become a serious threat for Europe in a warmer climate. The strong similarity between the observed and simulated storms supports the physical arguments for this statement.

Keywords Cyclones · North Atlantic · Extratropical Transition · Reanalysis

M. Dekker
Royal Netherlands Meteorological Institute KNMI, POBOX 201, 3730 AE De Bilt, Netherlands.
Institute for Marine and Atmospheric Research Utrecht, University of Utrecht, Netherlands. E-mail: m.m.dekker1@students.uu.nl

R. Haarsma
Royal Netherlands Meteorological Institute KNMI E-mail: haarsma@knmi.nl

H. de Vries
Royal Netherlands Meteorological Institute KNMI E-mail: vries@knmi.nl

A.J. van Delden
Institute for Marine and Atmospheric Research Utrecht, University of Utrecht, Netherlands. E-mail: a.j.vandelden@uu.nl

M. Baatsen
Institute for Marine and Atmospheric Research Utrecht, University of Utrecht, Netherlands. E-mail: m.l.j.baatsen@uu.nl

1 Introduction

Hurricane-force winds pose a significant threat to coastal regions, inflicting severe damage to infrastructure and agriculture (Dorland et al, 1999). In the North Atlantic, most hurricanes ($>$ Beaufort 12) originate and stay near the Caribbean sea, the Gulf of Mexico or along the eastern coast of the United States. Only a few hurricanes actually reach Europe. The question of whether this will change in the future has been debated. Recent research suggests that climate warming causes a poleward and eastward extension of the hurricane genesis area (Zhao and Held, 2012; Murakami et al, 2012). However it is uncertain whether these changes and the increase in sea surface temperatures (SSTs) are large enough to enable hurricanes to enter Europe. Recent studies have shed some light on this debate. Using a high resolution (˜25 km grid size) global climate model, Haarsma et al (2013) showed that the frequency of hurricane-force winds will increase considerably in Europe by the end of the twenty-first century. They suggested that higher SSTs and extension of the hurricane breeding ground imply that tropical cyclones are more likely to reach the midlatitudes before they dissipate, which will facilitate reintensification through merging with a baroclinic wave. Baatsen et al (2015) subsequently showed for these model simulations that a large percentage of future cyclones that enter Europe reattain a lower warm core and that a pronounced part of these so-called warm seclusions upholds a sting jet. As these cyclones pose a threat to Europe, it is crucial to assess whether observation-based analysis of the development of the cyclone structure lends further support to the key result of Baatsen et al (2015), specifically that warm seclusion cyclones typically produce the strongest winds. This is the focus of this paper.

Concerning structural development, extratropical transition is a major feature in cyclones from low-latitudes to eventually enter Europe. Of the North-Atlantic tropical cyclones, 46% undergoes extratropical transition (Hart and Evans, 2001), which includes changes to the structure of the cyclone, such as asymmetries in wind, thermal structure and moisture field (Klein et al, 2000). This transition is the consequence of the interaction of the northward propagating tropical cyclone with the midlatitudinal environment, which may include the presence nearby troughs, increased baroclinicity, vertical shear, cooler SSTs and strong SST gradients (Jones et al, 2003).

Analyses of cyclone life cycles have been done in various ways. For example, Agusti-Panareda et al (2004) described three different stages in their study of hurricane *Irene* (1999): the tropical stage, the transformation stage and the extratropical stage (complementary to the two stages used in Klein et al (2000)). This has the potential of describing different parts of a particular cyclone evolution, but does not qualitatively distinguish one cyclone life cycle from another. Hart (2003) proposed a three-dimensional cyclone phase space using relative thickness symmetry, which is a measure of frontal nature of the cyclone and the vertical derivative of the horizontal height gradient (at two different atmospheric layers), which is a measure of the thermal wind and thus the thermal nature of the core. Using this phase space analysis, Hart showed the potential to distinguish different cyclone life cycles and therefore to categorize these life cycles. Hart (2003) used NCEP-NCAR reanalyses to examine a large number of storms and subsequently described different kinds of life cycles using cyclone examples. This paper extends the research on cyclone life cycles, by focusing on storms that enter Europe. An important question is whether a connection exists between the cyclone life cycle and cyclone strength, and if so, what physical processes are behind this connection.

In this paper the MERRA reanalysis for the period 1979-2013 is used (details of this dataset will be given in section 2). This data set, together with the analysis tools, is described in the methodology section. To distinguish and classify the different life cycles of those cyclones that enter Europe, the phase space analysis of Hart (2003) is used. This is discussed in the methodology (section 2), together with the cyclone tracking and the indices for baroclinic instability. Section 3 contains the actual classification based on the mentioned phase space analysis. In section 4 the structural evolution of the different life cycles is described. Section 5 contains the conclusions and a discussion with respect to the impact of global warming.

2 Methodology

2.1 Model specifications

For this study the MERRA reanalysis of the Global Modeling and Assimilation Office (GMAO) has been used, which is conducted with version 5.2.0 of the GEOS-5 ADAS. The resolution of the MERRA dataset is 0.66° longitude by 0.5° latitude and it has 72 vertical layers. For the analysis the vertical resolution has been interpolated to an equidistant resolution of 17 layers of 50 hPa from 1000 to 200 hPa, similar as in Hart (2003).

2.2 Cyclone detection and tracking

The analysis period is 1979-2013 for the months of August through November, which covers the main hurricane season. Cyclone tracking is done for the region 100°W-40°E and 0°N-90°N. Around local 10 m wind maxima (found using the threshold of $\geq$ 14 m s^{-1}), the lowest sea level pressure within a 10° range is defined as a cyclone center. The threshold of $\geq$ 14 m s^{-1} is intentionally chosen relatively low to prevent gaps in the tracking of cyclone. The 10° range around the wind maximum prevents a single storm's location to be counted twice.

To track cyclones, the detection described above will be done at each timestep (Δt = 1h) and the given pressure minima will be automatically linked to a past pressure minimum if it is within 10° range of a pressure minimum one timestep later. A newly found pressure minimum may be linked to a past pressure minimum up to 16 hours back. In some cases, corrections had to be done manually, for example if two systems merge or if a cyclone starts following the track of a nearby other storm. These corrections are based on horizontal 850 hPa equivalent potential temperature (θ_E) and sea level pressure (p) fields. After the tracking of the cyclones the following selection criteria are used:

- At least once throughout the cyclone life cycle, the cyclone attains a wind speed of at least Beaufort class 8 (>17.2 m s^{-1}).

- The cyclone is tracked over a period of at least three days.
- The cyclone originates from latitudes equatorward of 37.5°N. This criterium selects those of tropical origin. The specific value of 37.5°N is based on the fact that extratropical transition occurs at 30°N-35°N during early and late hurricane season and at 40°N-50°N during peak of hurricane season (Hart and Evans, 2001).
- The cyclone reaches Europe, which is defined as 15°W - 40°E by 37.5°N - 90°N (indicated in Fig. 4).

2.3 Phase space analysis

The phase-space analysis by Hart (2003) is used to describe the cyclone structure and its evolution. This analysis involves three parameters: thermal symmetry (B) of the cyclone and the lower and upper cyclone thermal wind (T_L and T_U). Below we briefly outline these three parameters. For a more detailed description we refer to Hart (2003). The thermal symmetry B is computed by the difference of the geopotential height averaged over two semicircles with a radius of 500 km around the cyclone center:

$$B = h(\overline{Z_{600\text{ hPa}} - Z_{900\text{ hPa}}}\,|_R - \overline{Z_{600\text{ hPa}} - Z_{900\text{hPa}}}\,|_L) \tag{1}$$

where h is an integer of value +1 for Northern Hemisphere, Z the geopotential height and the subscripts R and L indicate the semicircles right and left of the propagation direction, respectively. Near-zero values of B indicate a thermally symmetric or tropical character, while high values indicate a thermally asymmetric character, which is often extratropical. Generally, the threshold for determining whether the cyclone is symmetric or asymmetric is 10 m (Hart and Evans, 2001; Hart, 2003).

The lower and upper thermal wind (T_L and T_U) are computed for the 900-600 hPa and 600-300 hPa layers respectively:

$$\mathrm{T}_L \equiv -|V_T^L| = \left.\frac{\partial(\Delta Z)}{\partial \ln p}\right|_{900hPa}^{600hPa} \tag{2}$$

$$\mathrm{T}_U \equiv -|V_T^U| = \left.\frac{\partial(\Delta Z)}{\partial \ln p}\right|_{600hPa}^{300hPa} \tag{3}$$

where p is pressure and $\Delta Z = Z_{max} - Z_{min}$, where Z_{max} and Z_{min} are the maximum and minimum geopotential height at a specific pressure level within the 500 km radius of the cyclone center. To get the average value of ΔZ over the specified pressure ranges, a linear regression of the ΔZ and $\ln p$ data is made with a vertical resolution in p of 50 hPa. The angle of this linear regression is used as the derivative of ΔZ to $\ln p$. Positive (negative) values of T_L or T_U indicate cores that are warm (cold) compared to the environment. This is because the cyclone height perturbation (ΔZ) is proportional to the geostrophic wind (Hart, 2003), and the derivative to p then basically is an expression for a scaled thermal wind magnitude, which is positive (negative) for a warm (cold) core.

In addition to these three parameters the cyclone size is computed, which is defined by the mean distance of the gale force wind field edge (16.9-18.5 m s^{-1}) towards the center of the cyclone.

2.4 Baroclinic instability

Baroclinic instability is often expressed by the Eady index (Hoskins and Valdes, 1990):

$$\sigma = 0.31\frac{f}{N}|\frac{\partial u}{\partial z}|, \tag{4}$$

where f is the Coriolis parameter, u the zonal wind and $N^2 = \frac{g}{\theta}\partial\theta/\partial z$ the Brunt-Väisälä frequency in which θ is the potential temperature and g the gravitational constant. Using the thermal wind balance and changing to pressure coordinates, the Eady index can be rewritten as $\sigma = 0.31\frac{g}{N}|\frac{\nabla\theta}{\theta}|$, where now $N^2 = -g^2\frac{\rho}{\theta}\partial\theta/\partial p$ (with ρ the density). In regions where $N^2 \leq 0$ there is convective instability.

The Eady index is a measure for the slope of the isentropes (surfaces of constant θ). Vertical displacements in a dry atmosphere are only baroclinically unstable if the slope of their movement is smaller than the slope of the basic state. However, we study systems that include moisture. A consequence of the air being moist is that it reduces the stability, as the air may release latent heat through condensation in the ascending branch of developing baroclinic waves. Therefore, the relevant slopes for instability are those of the equivalent potential temperature (θ_E) which takes into account the change in temperature due to the release of latent heat. For moist systems, such as tropical cyclones, we argue that baroclinic instability is better represented by a moist Eady index $\sigma_m$in which θ is replaced by θ_E:

$$\sigma_m = 0.31\frac{g}{N_e}|\frac{\nabla\theta_e}{\theta_e}|, \tag{5}$$

where N_e is the Brunt-Väisälä frequency using the equivalent potential temperature $\theta_e = \theta \cdot e^{L_v r_s/c_p T}$. L_v is the latent heat of evaporation, r_s the saturation mixing ratio, c_p the heat capacity of dry air and T the absolute temperature, resulting in $N_e = \sqrt{-g^2\frac{\rho}{\theta_e}\frac{\partial\theta_e}{\partial p}}$.

3 Classification of cyclone life cycles

The cyclone tracking algorithm outlined in section 2.2 on the MERRA data provides a set of 53 cyclones. Originating from latitudes equatorward of 37.5°N, these cyclones encounter different physical circumstances when crossing the North Atlantic and undergo various kinds of structure evolution before reaching Europe. Using the phase-space analysis of Hart, four physically distinct life cycle classes have been identified. These life cycle classes describe the different possible transitions a cyclone may undergo when entering the midlatitudes. In the classification we have been guided by the known structure evolutions that that have been described in the literature (Hart, 2003; Hart and Evans, 2001; Jones et al, 2003; Maue, 2010). The four classes are described below.

Table 1: Characteristics of the four different life cycle classes, showing number of storms, average pressure minimum and average wind maximum (shown with standard deviations). The last column shows the latitude where they enter Europe (i.e. entering rectangle 15°W by 37.5°N). The warm seclusion life cycle has been subdivided into two classes (see 4.2). *ETT is an abbreviation for extratropical transition.

	Class	Amount	$\overline{p_{min}}$ (hPa)	$\overline{v_{max}}$ (m s^{-1})	Enter Europe
a.	Tropical cyclone life cycle	8 (15%)	977±9	21.9±1.7	52°
b.	Extratropical cyclone life cycle	7 (13%)	970±13	21.5±2.3	58°
c.	Classic ETT* cyclone life cycle	10 (19%)	972±7	22.5±1.7	55°
d.	Warm seclusion (WS) life cycle	28 (53%)	963±13	22.5±2.4	53°
	- Extratropical WS life cycle	17 (32%)	967±14	21.6±2.2	51°
	- Tropical WS life cycle	11 (21%)	958±13	23.9±2.1	58°
	Total	53 (100%)	968±13	22.2±2.1	54°

3.1 Symmetric warm-core development: Tropical cyclone life cycle

Cyclones with tropical characteristics can be characterized by a thermally symmetric or non-frontal structure ($B < 10$ m) and a warm core ($T_L > 0$, $T_U > 0$). Cyclones of the tropical life cycle start with these characteristics. The lower-troposphere warm core increases upwards due to sustained convection (Hart, 2003). Combined with subsidence within the eye, a deep warm core (high T_U and T_L) is established, visible at the start of Fig. 2a. Because, by selection, all systems move across the North-Atlantic into Europe, these cyclones are subject to decreasing SSTs and lose their warm-core structure. The fact that these cyclones do not develop thermal asymmetry (B remains < 10 m) can be explained by that they are not subject to strong vertical shear, trough interaction or baroclinicity. In the early phase of this life cycle, the cyclone's spatial extent is usually small (200-400 km), which steadily grows in time. The pressure minimum is in some cases found early in the life cycle during tropical intensification, but in other cases it is found near the point where the cyclone, after attaining a deep cold-core structure that has been developed over cold SSTs, re-establishes a shallow warm core.

We find that about 15% of the observed cyclones show this life cycle. These cyclones tend to enter Europe in France and Great-Britain and never attain latitudes higher than 60°N. The average wind speed maximum and average pressure minimum of this class are 21.9±1.7 m s^{-1} and 977±9 hPa, respectively, which makes this the weakest class of low-latitude originating storms entering Europe (see Tab. 1).

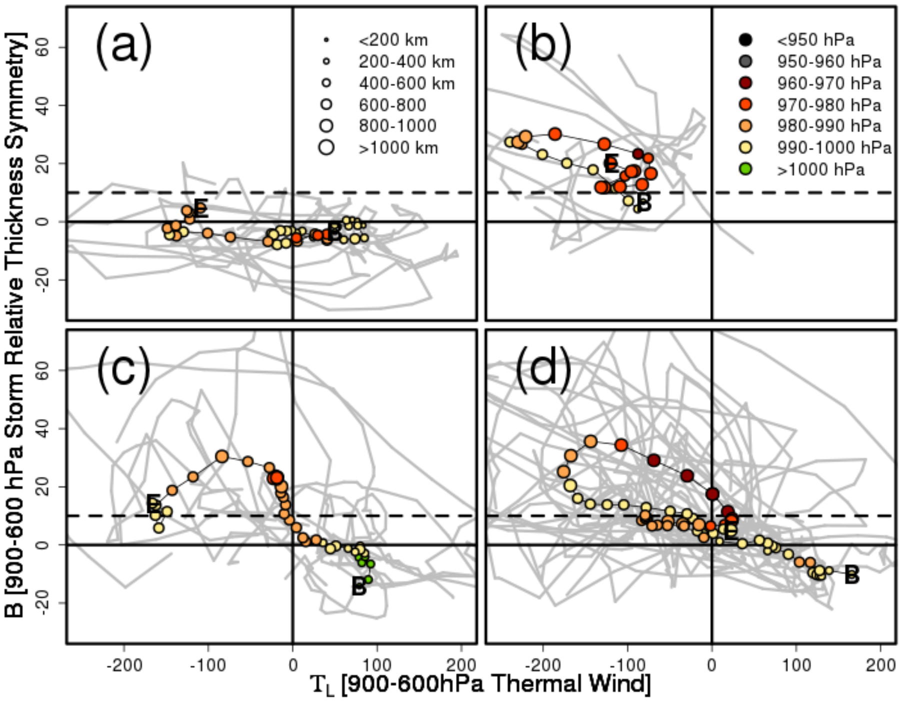

Fig. 1: Diagrams showing the composite thermal symmetry (m) and thermal wind at 900-600 hPa ($m^2s^2kg^{-1}$)for different cyclone life cycle classes: tropical life cycle (a), extratropical life cycle (b), classic ETT life cycle (c), warm seclusion life cycle (d). Composition is made by averaging around the pressure minimum, with the minimum averaging of at least three cyclones. Colors indicate central mean sea level pressure and dot size indicates system size, based on mean radius of gale force winds (17 m s^{-1}). Grey shaded lines show all the single life cycles of that class. A 24 h running mean has been used for all graphs. Timestep in composite figures is 6 hours. Capitals B and E in the figures point to the beginning and end of the life cycle. Dashed horizontal line shows the threshold value of $B = 10$ m.

3.2 Asymmetric cold-core development: Extratropical cyclone life cycle

The cyclones pertaining to the extra-tropical life cycle originate with a cold-core structure (T_L <0, T_U <0) (Fig. 2b) and retain it throughout their development in combination with a strong thermal asymmetry (B>10) (Fig 1b). Although coming from below 37.5 N, these are the characteristics of an extratropical cyclone. Often visible in these cyclone life cycles is an increase of the cold-core structure in an early phase, which is reflected by T_L becoming increasingly negative. The middle- and upper-tropospheric height gradients above the surface cyclone then intensify (isobaric heights decrease) more rapidly than near the surface, leading to an increasing cold-core cyclone signature. With B increasing, thermally direct circulation dictates that cold air is advected in the rear of the cyclone and warm air is advected further north, sustaining the strongly negative T_L . This is often followed by an increase of T_L as can be seen in Fig. 1b and Fig. 2b, where also an increase in pressure is clearly visible. For detailed analyses of this life cycle, see Hart et al. (2003). Occlusion (following the

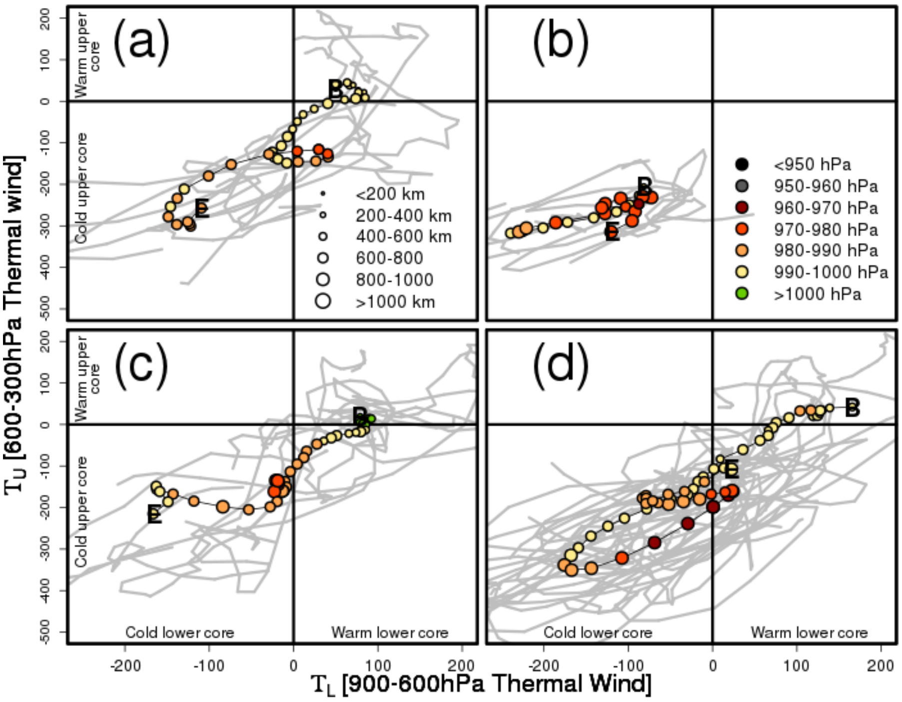

Fig. 2: As Figure 1 but now for the thermal wind at 900-600 hPa and at 600-300 hPa for different cyclone life cycles.

Norwegian cyclone model) of the cyclone fronts can be recognized by re-establishing thermal symmetry in the latter phase of the cyclone life cycle. If the cyclone does not interact with another trough or is not subject to increased surface fluxes, further intensification stops and the cyclone decays. The radius of the system (mean gale force wind radius) is relatively large throughout the extratropical cyclone life cycle (Fig. 2b).

About 13% of analyzed cyclones endure an extratropical life cycle. These cyclones tend to penetrate further north than cyclones with a tropical life cycle, reaching Europe at the northernmost point of Great Britain or even near Iceland. The average wind speed maximum and average pressure minimum of this class are 21.5±2.3 m s^{-1} and 970±13 hPa, respectively, which makes these storms of moderate strength among the low-latitude originating storms entering Europe (see Tab. 1).

3.3 Extratropical transition: Classic ETT cyclone life cycle

The first two classes mentioned above (tropical and extratropical cyclone life cycles) are called conventional or single phase life cycles as they do not undergo major phase transitions in thermal symmetry and thermal wind (Hart, 2003). The remaining two classes do undergo major phase transitions and differ in the experienced forcing mechanisms throughout their life cycle.

One of these major phase transitions is extratropical transition (ETT), changing the warm-core symmetric structure of a tropical cyclone into the cold-core asymmetric structure of an extratropical cyclone (Jones et al, 2003). The tropical origin is visible in Fig. 1c, with near-zero or even negative values of B and positive values of T_L . This is called the tropical stage. One would expect to find positive values of T_U , too, which is on average not the case (Fig. 2c). This depends on the maturity of the tropical cyclone. Some do start with a positive T_U , while others do not as can be seen from the individual life cycles in Fig. 2c. In this tropical stage, the cyclone radius is relatively small but slowly increasing, similar to the early phase of the tropical (conventional) life cycle. We adopt the criterion Hart (2003) proposed for the onset time of the ETT, when B exceeds 10 m, which corresponds to the cyclone entering a baroclinic environment (Hart, 2003; Klein et al, 2000). The value of $B = 10$ m is marked in Fig. 1c.

After the ETT, in the second transformation or hybrid stage, the cyclone interacts with its new environment, which usually consists of merging with an extratropical system or upper-level trough. During this stage, the tropical cyclone generally develops an increased translation speed. In the early stages of ETT, the cyclone tends to weaken first (Hart and Evans, 2001), which could be attributed to the interaction between the cyclone and an upper-level trough, as this is associated with high vertical wind shear. The decrease in intensity of the cyclone also depends on the inner-core convection evolution by the environmental changes (Jones et al, 2003). Important changes after an ETT are the loss of organized convection in the inner core, the increase in translation speed, the loss of upper-level outflow circulation, increased frontogenesis, cyclone vertical tilt, asymmetry in the precipitation, moisture and temperature fields and the expansion of the gale force winds area (Hart and Evans, 2001). Throughout the ETT, some cyclones directly attain a lower cold core and a thermally asymmetric structure ($B > 10$ m; Fig 1c). However, ETT as it is described in Hart (2003), implies first a transition to the upper-right quadrant in Fig. 1c. The the individual cyclone life cycles depicted in grey reveal that indeed many of them undergo this transition. This quadrant refers to the so-called hybrid stage, where a lower warm core ($T_L > 0$) pertains in a baroclinic environment ($B > 10$ m). The latent heat release possible in the warm-core structure of the cyclone during this phase, may contribute to a deepening. The end time of the hybrid stage (T_L becomes negative) is sometimes referred to as the end of the ETT (Hart and Evans, 2001). The duration of the hybrid stage differs among cyclones. The extratropical stage contains the decay and sometimes a reintensification of the cyclone. Both weak and strong cyclones can reintensify, but weak cyclones need to have a smaller duration of the hybrid stage for them to survive longer. The pressure evolution is therefore determined by weakening in an early phase of the ETT, the intensification during the hybrid stage (of cyclones that have one), and possible reintensification after the ETT (see Fig. 1c). Cyclones of this life cycle fade as cold-core, thermally asymmetric cyclones.

About 19% of the observed cyclones follow this life cycle. The tracks of these cyclones start relatively deep in the tropics. They usually arrive in Europe around Great Britain. The average wind speed maximum and average pressure minimum of cyclones of this class are 22.5±1.7 m s^{-1} and 972±7 hPa, respectively, which is relatively weak (Tab. 1).

3.4 Transition to warm seclusion: Warm seclusion life cycle

Finally, more than 50% of the storms undergo another major transition and become what is known as a warm seclusion storm. A warm seclusion occurs, when during the bending of the cold and warm front, part of the cold front gets separated from the cyclone center and propagates eastwards, perpendicular to the warm front (Shapiro and Keyser, 1990). This process is called a frontal T-bone fracture. This is associated with trapping of warm air (the so-called bent-back warm front) in the core of the cyclone. A large part of the analyzed cyclones that attain a warm seclusion structure start with a warm T_L and a symmetric structure as seen in Fig. 1d and 2d. In their path towards Europe they lose their warm core structure and become asymmetric. During this transition they weaken. What distinguishes this life cycle from the classic ETT life cycle is that after this transition, due to the seclusion, a warm core is re-established again. This is caused by the release of latent heat and advection within the warm conveyor belt. The warm seclusion is often accompanied by a rapid intensification because both baroclinic processes and latent heat release contribute to the development of the storm. The average deepening is about 30 hPa in two days. The minimum pressure is attained when the warm seclusion is completed. Thereafter the cyclone tilt disappears and they lose their warm core before they fade away. This structure development is dominant for the storms that reach Europe. Moreover, the warm seclusion life cycle class contains the strongest storms that originate in the tropics. Eight out of the ten strongest storms are all warm seclusion storms. Also, on average they are the strongest storms with an average wind speed maximum of 22.5±2.4 m s^{-1} and average pressure minimum of 963±14 hPa.

3.5 Summary

We have divided the cyclones that reach Europe and originate from lower latitudes in four different classes based on the characteristic pathways in the Hart diagrams. Each of these classes describes a physically different life cycle. The life cycles of the individual cyclones shown in Fig. 1 and 2, support this classification. The four possible life cycles are schematically represented in Fig. 3, and correspond to the physical processes and transitions that cyclones may experience when they enter the midlatitudes with colder SSTs.

The minority of the cyclones experience small structure transitions (tropical and extratropical life cycle, 28% in total), but the majority (72%) undergoes major transitions in cyclone structure like extratropical transition and warm seclusion. Intensification of these cyclones mainly appears in the form of a reintensification at midlatitudes while warm seclusion intensification generates the lowest pressure values.

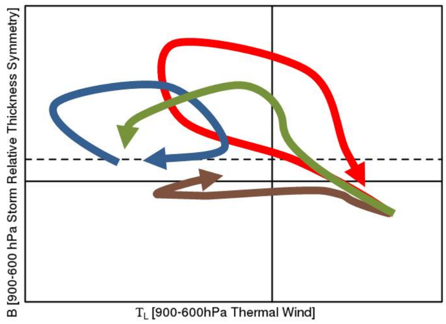

Fig. 3: Schematic picture showing the different cyclone stages within the cyclone life cycles. The blue line represents the extratropical life cycle, brown the tropical life cycle, green the extratropical transition life cycle and red the warm seclusion life cycle. Dashed line represents the threshold value of $B = 10$ m.

4 Comparison of life cycles in structure and development

Below we will further investigate the structure and the development of the four different classes. Because the warm seclusion storms are the largest and strongest of the four classes that reach Europe, thereby being a potential risk for society, we will focus on the differences of these storms with respect to the other classes. The relative importance of warm seclusion storms is also motivated by the study of Baatsen et al (2015), which suggests that those storms will increase in frequency and strength in a future warmer climate, arriving in Europe possibly with hurricane force wind.

This section will first elaborate on the cyclone structure, followed by an analysis of the development of θ_E at 850 hPa, sea level pressure and the Eady growth parameter σ_m at 500 hPa.

4.1 Cyclone structure

The cyclone structure is analyzed at the pressure minimum point in time because it is both a physical well-founded point in the life cycle to compare different cyclones and because the warm secluding process is usually just prior to the pressure minimum, which will allow for the warm seclusion features to be visible at this point. Figure 4 shows the trajectories of the warm seclusion cyclones together with the location of the minimum pressure. It reveals that the minimum pressure is mostly attained during the later phase of their life cycle, and often within the European domain. The composite tracks of the four different life cycles (lower right panel Fig. 4) reveal that the warm seclusion storms have longest tracks starting in the deep tropics and penetrating far into Northern Europe.

Figure 5 shows the composite structures of the four cyclone life cycles at the time when central sea level pressure is at a minimum. A first observation is the overall lower θ_E in the warm seclusion panel with respect to other classes, which is mainly because of the relatively late moment and more northward location at which these cyclones intensify. Comparing the θ_E structure of these cyclones further with that

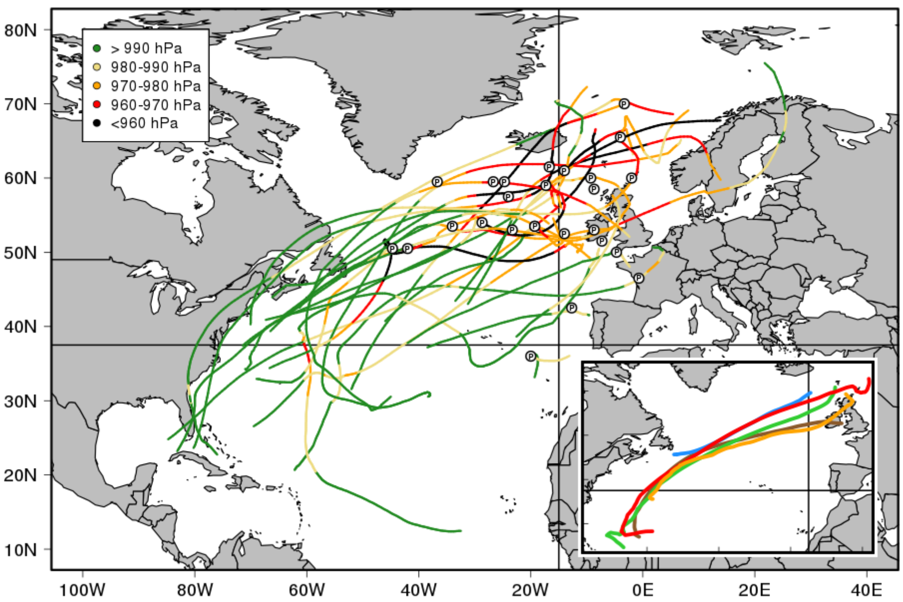

Fig. 4: Tracks of the warm seclusions. Large white dots marked with *P* indicate the points of minimum pressure. Colors indicate pressure. Hourly data is shown, with a running mean of 24 hours. The frame on the lower right shows the composite (24 h running mean-) tracks of the different life cycles: tropical life cycle (brown), extratropical life cycle (blue), classic ETT life cycle (green), extratropical warm seclusion life cycle (orange) and tropical warm seclusion life cycle (red). Averaging done around the point at which the tracks enter Europe with a minimum amount of three cyclones. Notable is that the average extratropical life cycle (blue in lower right panel) does not cross 37.5°N, which is due to the high track variability in the individual tracks.

of other cyclone life cycles, the main characteristics are the consistency of the figure, the curled warm conveyor belt (WCB), the eastward progressing cold front and the vertically stacked wind pattern, indicated here by the colocation of the maximum windspeed at 10 m, 850 hPa and 250 hPa. The smoothness of Fig. 5d points to the consistency in the structure of warm seclusions at their highest intensity, which is not the case for the other life cycles. Additionally, the curled WCB displaying a well-defined comma shape is also quite unique to the warm seclusion life cycle. The eastward progressing cold front in Fig. 5d is more strongly present than in any other cyclone life cycle pressure minimum. In analogy with the curled WCB, the cold front progresses far east, which is characteristic for the T-bone fracture. The intensity of the cyclone at this point in time, the far propagated low-θ_E region and vertically homogeneous eastward winds south of the cyclone may point to the presence of a dry intrusion.

4.2 Development of θ_E, p and σ_m

The variables θ_E, sea level pressure and the moist Eady growth rate σ_m at the cyclone core provide information about the development of the cyclone and the specific

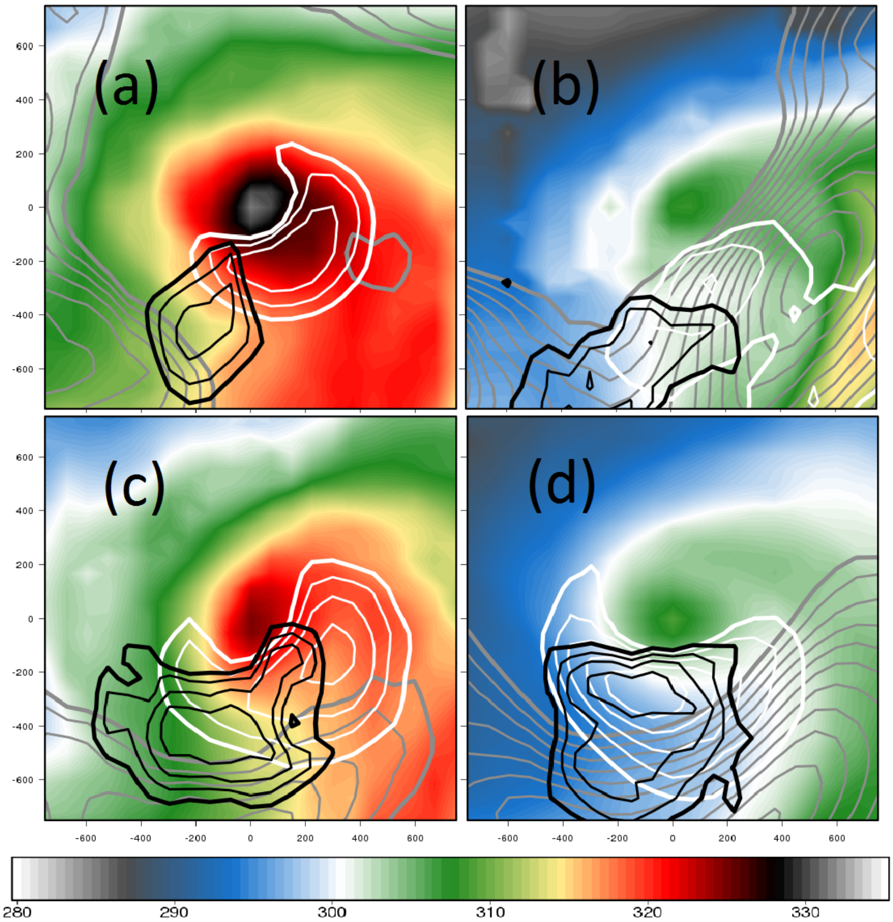

Fig. 5: Composites of equivalent potential temperature (shaded in K) at 850 hPa in horizontal cross-sections of cyclone cores during the time when the central sea level pressure is at its minimum. The four panels show the different life cycles: tropical life cycle (a), extratropical life cycle (b), ETT life cycle (c) and the warm seclusion life cycle (d). Thick contour lines show wind speed: 14 m s^{-1} at 10 m (black), 25 m s^{-1} at 850 hPa (white) and 30 m s^{-1} at 250 hPa (gray). Thin contour lines show contours of 0.5 m s^{-1} at 10 m (black) and 2 m s^{-1} at 850 and 250 hPa (white and gray). Horizontal and vertical axes show distance w.r.t. the cyclone center in km.

phases the cyclone is in. High values of θ_E allow for stronger latent heat driven deepening as occurs in tropical cyclones, while σ_m is a measure of baroclinic instability, which is the major energy source for extratropical cyclones.

More than half of the warm seclusion storms, although originating south of 37.5°N, do not start with a tropical structure that is characterized by a warm core and a non-frontal structure, but already possess extratropical characteristics. Although they are almost indistinguishable in their final warm seclusion structure, the different origin has implications for their ultimate pressure minimum and the development of θ_E and σ_m. We therefore divided the warm seclusion life cycle in two sub-cycles: warm

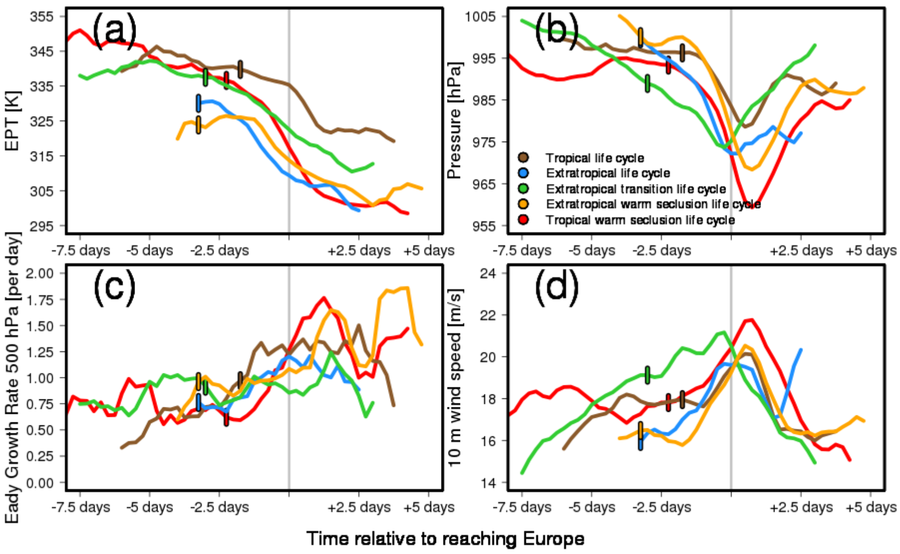

Fig. 6: Development of θ_E at 850 hPa (a), sea level pressure (b), the moist Eady growth rate σ_m at 500 hPa (c) and 10 m wind speed (d) at the cyclone center for every life cycle class. Averaging done around the minimum central sea level pressure along the cyclone track, with a 12 h running mean. The grey bar shows the moment at which these storms (in average) arrive in Europe, and the small vertical colored bars show the moment at which cyclones from that particular class in average cross 37.5° latitude. Averages of at least three cyclones are shown. The colors are analogous to the lower right frame in Fig. 4.

seclusions that originated as tropical cyclones, i.e. following ETT, called tropical warm seclusions, and warm seclusions that originated as extratropical cyclones, i.e. without ETT, called extratropical warm seclusions.

Figure 6a shows the θ_E development of the cyclone life cycles. Cyclones that originated as tropical cyclones start with higher values of θ_E than their extratropical originating counterparts. The tropical warm seclusions lose rather much of their θ_E when they enter Europe. However, together with the extratropical warm seclusions they survive longest in Europe, up to more than 5 days. The large reduction of θ_E of the tropical warm seclusions could be explained by the fact that they travel relatively high northward.

The sea level pressure development for each cyclone life cycle is shown in Fig.6b. It reveals that both warm seclusion life cycles have their pressure minimum latest of all, about a day after entering Europe, while other cyclone life cycles have this minimum close to the time they enter Europe. Striking is the strong deepening rate of the warm seclusions, both starting a day prior to the entering of Europe. The tropical warm seclusion storms attain the lowest pressure with an average value of about 960 hPa. Notable is the extensive length of the tropical warm seclusion cycle prior to entering midlatitudes. Together with the extensive lengths of the extratropical transition life cycle and the tropical life cycle this is in clear contrast with the short tropical history the two other life cycles have; the extratropical warm seclusion life cycle and the extratropical life cycle. This confirms the rather different origin these cyclones have, although they all come from latitudes lower than 37.5°N. In Fig. 6b and d, for the tropical warm seclusions, a slight minimum in pressure and maximum in wind speed can be distinguished roughly 6 days prior to the entering of Europe. This may refer to the tropical intensification of these cyclones prior to entering midlatitudes, but the signal is diffused due to the averaging of the individual evolutions. The midlatitude intensification and the loss of θ_E in tropical warm seclusions occur roughly at the same time, perhaps both influenced by ETT, which increases cyclone speed and therefore the rate at which its environment becomes colder. This may also enhance the intensification.

Figure 6c shows the moist Eady growth parameter σ_m. Being a measure of baroclinic instability, an increase of it after the entering of midlatitudes is expected. Remarkable is the increase in σ_m of the tropical warm seclusions around their arrival in Europe, reaching the highest values during their lowest core sea level pressure. This indicates that moist baroclinic instability increases during ETT and the forming of the warm seclusion for this cyclone life cycle. A similar behavior is observed for the extratropical warm seclusions. Having these maxima in σ_m near their moments of highest intensity, makes the warm seclusions rather unique with respect to other cyclone life cycles, which do not have such maxima. It points toward the important role of moist baroclinic instability for the warm seclusions during their reintensification and being responsible for their relative strength.

5 Summary and Conclusions

Using the MERRA reanalysis for the period 1979-2013 we have analyzed the characteristics of 53 cyclones originating from the tropics that reach Europe. These characteristics have been classified into four classes based on the pathways in the phase space diagrams of Hart (2003). The classes describe the transitions cyclones undergo and the characteristic phases such as tropical, extratropical or hybrid they experience. These life cycles vary in trajectory and intensity. Of those four classes, warm seclusions obtain the highest intensity in pressure and wind speed. At the time of their minimum sea level pressure, warm seclusions reveal a consistent structure consisting of a far eastward moving cold front, a northwestward curling WCB and the effects of dry intrusion. These features are almost non-existent in the other cyclone life-cycle types investigated in this study. Of the warm seclusions the subclass of tropical warm seclusion storms attain the lowest pressure and show the fastest re-deepening rates. Both baroclinic instability and release of latent heat contribute to the strong reintensification of these storms. The pressure minima of warm seclusions occur relatively late comparing to other cyclone life cycles, about a day after entering Europe adding to the potential threat for Europe of these systems.

Baatsen et al (2015) have suggested in a model study that tropical warm seclusions are the strongest tropical storms of the ones that reach Europe. Our observational study confirms this hypothesis. The structural development of the observed storms reveals large similarity to that described in Baatsen et al (2015) (compare for example Fig. 4d of this article with Fig. 4a of the mentioned paper). According to these authors, the frequency and intensity of tropical warm seclusions will significantly increase in a warmer climate, with some of them reaching hurricane force when they enter Europe. The large similarity between the observed and modeled storms for the present climate increases the credibility of the projections made by Baatsen et al (2015), although many uncertainties remain, such as for instance the impact of mixing with the subsurface ocean resulting in cooler SSTs, which was not modeled in the AMIP simulations of Haarsma et al (2013).

Acknowledgements This paper was partly funded through the PRIMAVERA project under Grant Agreement 641727 in the European Commission's Horizon 2020 research programme.

References

Agusti-Panareda A, Thorncroft C, Craig G, Gray S (2004) The extratropical transition of hurricane Irene (1999): A potential-vorticity perspective. QJR Meteorological Society 130:1047–1074

Baatsen M, Haarsma R, Van Delden A, De Vries H (2015) Severe autumn storms in future Western Europe with a warmer Atlantic Ocean. Climate Dynamics 45:949–964, dOI: 10.1007/s00382-014-2329-8

Dorland C, Tol RSJ, Palutikof P (1999) Vulnerability of the Netherlands and northwest Europe to storm damage under climate change. Climate Change 43:513–535

Haarsma R, Hazeleger W, Severijns C, Vries H, Sterl A, Bintanja R, Oldenborgh G, Brink H (2013) More hurricanes to hit Western Europe due to global warming. Geophysical Research Letters 40:1–6

Hart R (2003) A cyclone phase space derived from thermal wind and thermal asymmetry. Monthly Weather Review 131:585–616

Hart R, Evans J (2001) A climatology of the extratropical transition of Atlantic tropical cyclones. Journal of Climate 14:546–564

Hoskins, Valdes (1990) On the existence of storm tracks. Journal of Atmospheric Science 47:1854–1864

Jones SC, Harr PA, Abraham J, Bosart LF, Bowyer PJ, Evans JL, Hanley DE, Hanstrum BN, Hart RE, Lalaurette F, Sinclair MR, Smith RK, Thorncroft C (2003) The extratropical transition of tropical cyclones: Forecast challenges, current understanding, and future directions. Weather and Forecasting 18:1052–1092

Klein P, Harr P, Elsberry R (2000) Extratropical transition of Western North Pacific tropical cyclones: An overview and conceptual model of the transformation stage. Weather and Forecasting 15(4):373–395

Maue RN (2010) Warm seclusion extratropical cyclones. Florida State University 1(3):33–52

Murakami H, Wang Y, Yoshimura H, Mizuta R, Sugi M, Shindo E, Adachi Y, Yukimoto S, Hosaka M, Kusumoki S, Ose T, Kitoh A (2012) Future changes in tropical cyclone activity projected by the new high-resolution MRI-AGCM. Journal of Climate 25:3237–3260

Shapiro MA, Keyser D (1990) Fronts, jet streams and the tropopause. In: Extratropical cyclones, the Erik Palmeén Memorial Volume, C W Newton and E O Holopainen, Am Meteorol Soc 1(3):167–191

Zhao M, Held I (2012) TC-Permitting GCM simulations of hurricane frequency response to sea surface temperature anomalies projected for the late-twenty-first century. Journal of Climate 25:2995–3009